Available online at www.sciencedirect.com
SCIENCE DIRECT®
Journal of Nuclear Materials 326 (2004) 86–96
journal of nuclear materials
www.elsevier.com/locate/jnucmat

Irradiation hardening behavior of polycrystalline metals after low temperature irradiation

T.S. Byun *, K. Farrell

Oak Ridge National Laboratory, Metals and Ceramics Division, P.O. Box 2008, MS-6151, Oak Ridge, TN 37831, USA

Received 26 September 2003; accepted 15 December 2003

Abstract

Irradiation hardening behaviors of body-centered cubic (bcc), face-centered cubic (fcc), and hexagonal close-packed (hcp) alloys and pure metals were characterized after neutron, or proton and neutron irradiations at low temperatures ($\leqslant 200$ °C). In the regression analysis, the radiation-induced increase in yield stress, $\Delta\sigma_{YS}$, was expressed in the form of a power law: $\Delta\sigma_{YS} = h(\text{dpa})^n$, where h and n are the regression coefficients and dpa is displacements per atom. The log–log plots of $\Delta\sigma_{YS}$ vs. dpa data showed two distinctive regimes: a low-dose regime where a rapid hardening occurs and a high-dose regime where the log–log plot shows a considerably reduced slope. Mean values for n obtained from the 19 metals were about 0.5 for the low-dose regime and about 0.12 for the high-dose regime. Some ductile metals like Fe, Cu and Zr displayed lower h and n values. Doses to reach the regime of reduced irradiation hardening, D_S, were in the range 0.003–0.07 dpa. Comparisons between radiation effect parameters led to a conclusion that the transition from the low-dose to the high-dose regime in irradiation hardening occurs either when the tensile specimen undergoes prompt plastic instability at yield or when saturation of defect cluster density occurs.

1. Introduction

Irradiation hardening in metallic materials is strong after irradiation at low temperatures (usually below 300 °C) because significant quantities of radiation-induced defect clusters are retained, and they impede the generation and glide of dislocations during deformation [1–4]. A great deal of effort has been made to explain the irradiation hardening behavior of metals, and to correlate the change in strength with the number density and size of radiation-induced defects and with irradiation dose [2,4–8]. Although there are multiple hypotheses concerning the mechanisms of irradiation hardening [6,7,9,10], the dose-dependence of the increase in yield stress, $\Delta\sigma_{YS}$, has been explored frequently using models based on barrier hardening theory [9,11].

Among the models for irradiation hardening, the simplest is in the form of the power-law expression:

$$\Delta\sigma_{YS} = h\phi^n, \tag{1}$$

where ϕ is the radiation fluence, which can be replaced by a factor related to defect cluster barriers, or by dpa (displacement per atom) [9,12–14]. At low doses, the exponent n has been measured to be about 1/2 for many metals [6,9,13–15], and 1/4–1/3 for copper and gold [12,15–17]. At higher doses, however, there is a tendency towards saturation in irradiation hardening, usually because of cascade overlap [18,19]. To consider the saturation region, Makin and Minter [5] suggested a two-parameter equation:

$$\Delta\sigma_{YS} = A[1 - \exp(-B\phi)]^{1/2}, \tag{2}$$

* Corresponding author. Tel.: +1-865 576 7738; fax: +1-865 574 0641.
E-mail address: byunts@ornl.gov (T.S. Byun).

0022-3115/$ - see front matter © 2004 Elsevier B.V. All rights reserved.
doi:10.1016/j.jnucmat.2003.12.012

where A and B are regression coefficients. Eq. (2) indicates a progressive transition from the low-dose regime, with $\phi^{1/2}$ dependence, to the saturation regime with an asymptotic value A at very high doses. In the present authors' earlier work on 3Cr, 9Cr, and A533B steels [14], however, the transition between the low-dose and the high-dose regimes was distinctive; a critical dose between the two regimes was determined without ambiguity, and the slopes of the log–log plots were distinctly different for the two regimes. This implies that there is a change in deformation mode and/or in defect-production behavior around the critical dose. The objective of this study is, therefore, to characterize the dose dependence of irradiation hardening using two power-law equations, and to explain the results in relation to the plastic deformation and defect-cluster accumulation behaviors.

Irradiation effects on the yield stress of 19 metals (10 bcc, 7 fcc, and 2 hcp metals) [20] were analyzed and compared. The log–log plots of $\Delta\sigma_{YS}$ vs. dpa data are presented for the 19 metals (24 cases). The coefficients of the power-law expression were obtained for both the low-dose and high-dose regimes, and the doses to saturation in irradiation hardening were determined. The critical doses to saturation in irradiation hardening and to plastic instability at yield are compared. Also, it is attempted to elucidate the relationships among material behaviors such as irradiation hardening, plastic instability, deformation mechanism, and defect-cluster number density.

2. Experimental

During the past several years, the authors have investigated the mechanical properties for many commercial and model alloys, and pure metals, after neutron or neutron and proton irradiation at low temperatures (under 200 °C). In the present study, the irradiation-hardening behavior of some 24 cases (19 metals) was analyzed. Table 1 includes the chemical compositions of the metals and their heat treatments, along with specimen types, SS-3, S-1, and BES/NERI types [14,21,22] and their gage section dimensions. Among the 19 metals, bcc metals consisted of 3 pure metals (Fe, Nb and V), a pressure vessel steel (A533B), a bainitic steel (3Cr–3WV), and 3 ferritic/martensitic (F/M) steels (9Cr–1MoVNb, 9Cr–2WVTa, 9Cr–2WV); fcc metals were 2 pure metals (Cu and Ni) and 5 austenitic stainless steels (316, 316LN, EC316LN, HTUPS316, and AL6XN); hcp metals were Zr and Zr-4.

Irradiation experiments were performed in the Hydraulic Tube facility of the High Flux Isotope Reactor (HFIR) at the Oak Ridge National Laboratory for fast neutron irradiations, and at the target area of the Los Alamos Neutron Scattering Center (LANSCE) accelerator at Los Alamos National Laboratory for high-energy proton and spallation neutron irradiations. Four of the 19 metals were irradiated in two or three irradiation experiments, making 24 cases in total. Irradiation doses achieved from the two facilities were 0–1.3 dpa from fast neutrons and 0–25 dpa from protons and spallation neutrons, respectively. Also, the irradiation temperatures in the two facilities were in the ranges 60–100 and 50–160 °C, respectively. The details of the irradiation conditions can be found in [14,21–23]. All tensile tests were conducted at room temperature in screw-driven machines at a nominal strain rate of about 10^{-3} s^{-1}. Irradiation and testing conditions, and baseline tensile data for the 24 cases, are listed in Table 2.

3. Results and discussion

3.1. Dose dependence of irradiation hardening

In Figs. 1–5, the dose dependencies of increase in yield stress, $\Delta\sigma_{YS}$ vs. dpa, are presented in the log–log format to reveal two distinct regimes, the low-dose and the high-dose regimes. Only representative trend lines are drawn for material groups to avoid being crowded, so the coefficients obtained for the trend lines may not be identical to those from regressions for individual cases, as listed in Table 3. For each regime, the regression curve of $\Delta\sigma_{YS}$ vs. dpa data was expressed in the form of the power law given by Eq. (1) [9,12]. The values for the coefficients h and n for both regimes are listed in Table 3, along with the values for the dose to saturation (or reduced rate) in irradiation hardening, D_S.

In Fig. 1 the $\Delta\sigma_{YS}$ vs. dpa data for bcc alloys are presented. Although the initial yield stresses of A533B steel, 440–500 MPa, were lower than those of the 3Cr and 9Cr steels, 540–570 MPa, the radiation-induced hardening was always higher in the A533B steel. It is clear that there exists a reduction in the slope of each log–log plot at a dose of about 0.04 dpa, at which the irradiation hardening changes from the low-dose regime to the high-dose (saturation) regime. As listed in Table 3, the values for the exponent n, representing the slopes of the log–log plots, ranged narrowly from 0.54 to 0.62 in the low-dose regime, and from 0.07 to 0.18 in the high-dose regime. With regard to the LANSCE-irradiated 3Cr and 9Cr steels, regression was not made for the low-dose regime because there were too few data belonging to the low-dose regime. In the high-dose regime, the exponents were the highest among the 3Cr and 9Cr steels, possibly because of additional hardening effects caused by helium bubbles [21,24]. A comparison between the data in Table 3 also indicates that the coefficient h, which represents the magnitude of irradiation hardening, was more material-dependent than the exponent n; higher h-values were obtained for the A533B

Table 1
Materials, heat treatments, and specimen types

No.	Materials	Chemical composition (wt%)	Heat treatment (in vacuum unless specified)	Specimen type[a]
1	A533B-a	Fe–0.22C–0.25Si–1.48Mn–0.52Mo–0.68Ni–0.018S–0.012P	Annealed at 880 °C for 4 h and air cooled, tempered at 660 °C for 4 h, reheat at 610 °C for 20 h	BES/NERI
2	A533B-b	”	”	SS-3
3	A533B-c	”	”	SS-3
4	3Cr–3WV	Fe–0.091C–0.3Mn–0.09Si–0.009S–0.015P–0.02Ni–3.05Cr–0.24V–0.02Cu–3.01W	Heated for 1 h at 1040 °C in flowing argon and cooled to room temperature in the cold zone; then reheated for 1 h at 760 °C and cooled	SS-3
5	9Cr–1MoVNb	Fe–0.09C–0.36Mn–0.08Si–0.004S–0.008P–0.11Ni–8.62Cr–0.98Mo–0.209V–0.063Nb–0.002Ti–0.013Co–0.03Cu–0.013Al–0.01W	”	SS-3
6	9Cr–2WVTa	Fe–0.11C–0.44Mn–0.21Si–0.015P–8.9Cr–0.01Mo–0.23V–0.012Co–0.03Cu–0.017Al–2.01W–0.06Ta	”	SS-3
7	9Cr–2WV	Fe–0.12C–0.51Mn–0.23Si–0.007S–0.014P–8.95Cr–0.01Mo–0.24V–0.012Co–0.03Cu–0.018Al–2.01W	”	SS-3
8	9Cr–2WVTa	Fe–0.11C–0.44Mn–0.21Si–0.015P–8.9Cr–0.01Mo–0.23V–0.012Co–0.03Cu–0.017Al–2.01W–0.06Ta	”	S-1
9	Mod. 9Cr–1Mo	Fe–0.092C–0.09Ni–8.32Cr–0.86Mo–0.48Mn–0.15Si–0.055N–0.06Nb–0.2V	”	S-1
10	Fe-a	(99.995% purity)	Annealed at 600 °C for 1 h	BES/NERI
11	Fe-b	Fe–0.013C–0.018Mn–0.018Ni (99.94% purity)	Annealed at 600 °C for 1 h	SS-3
12	Nb	Nb–0.3Si–0.01Ni–0.06Ni–0.05Ta–0.005C–0.001S (99.5% purity)	Annealed at 900 °C for 1 h	BES/NERI
13	V	V–0.026Si–0.039Mo–0.027O–0.0096N–0.0024C (99.8% purity)	Annealed for 30 min at 900 °C	BES/NERI
14	316-a	Fe–0.059C–1.86Mn–0.57Si–0.018S–0.024P–17.15Cr–13.45Ni–2.34Mo–0.1Cu–0.02Co–0.031N	Annealed at 1050 °C for 30 min	BES/NERI
15	316-b	”	”	SS-3
16	316LN	Fe–10.2Ni–16.3Cr–2.01Mo–1.75Mn–0.39Si–0.11N–0.029P	Annealed at 1050 °C for 30 min	SS-3
17	EC316LN	Fe–12.2Ni–17.45Cr–2.5Mo–1.81Mn–0.39Si–0.024C–0.067N	Annealed at 950 °C for 1 h	S-1
18	HTUPS316	Fe–16.2Ni–13.9Cr–2.46Mo–2.04Mn–0.12Si–0.076C–0.021N–0.15Nb–0.52V–0.27Ti	Annealed at 1200 °C for 12 min	S-1
19	AL6XN	Fe–24Ni–20.5Cr–6.3Mo–0.4Mn–0.4Si–0.02C–0.22N	Annealed at 1110 °C for 30 min	S-1
20	Cu	Cu–1.6S–0.09Cr–0.22Ni–0.1P–0.27Fe–4.8Ag	Annealed at 450 °C for 30 min	BES/NERI
21	Ni	(99.99% purity)	Annealed at 900 °C for 30 min	BES/NERI
22	Zr-4-a	Zr–1.4Sn–0.015C–0.1Fe–0.001S–0.06O–<0.1Ni-<0.001N	Annealed at 670 °C for 30 min	BES/NERI
23	Zr-4-b	”	”	SS-3
24	Zr	Zr–0.0058Hf–0.0056Fe (99.94% purity)	Annealed at 670 °C for 30 min	BES/NERI

[a] Gage section dimensions for SS-3, S-1, and BES/NERI types are $0.76\times1.52\times7.62$, $0.25\times1.2\times5$, and $0.25\times1.5\times8$ mm^3, respectively.

steel cases. For 3Cr, 9Cr, and A533B steels, the doses to saturation in irradiation hardening, D_S, were in the range 0.03–0.05 dpa, with an average of 0.04 dpa.

Pure bcc metals also showed a clear transition in the dose dependence of $\Delta\sigma_{YS}$, as seen in Fig. 2. Two Fe cases showed similar irradiation hardening behaviors in spite

Table 2
Irradiation conditions, testing conditions, and baseline tensile data

No.	Materials	Crystal structure	Irradiation facility	Dose range (dpa)	Irradiation temperature (°C)	Test temperature (°C)	Yield stress (MPa) (0 dpa)	Uniform elongation (0 dpa)
1	A533B-a	bcc	HFIR	0–0.89	60–100	25	497	0.13
2	A533B-b	bcc	HFIR	0–1.2	60–100	25	444	0.10
3	A533B-c	bcc	HFIR	0–1.28	60–100	25	447	0.11
4	3Cr–3WV	bcc	HFIR	0–1.2	60–100	25	546	0.08
5	9Cr–1MoVNb	bcc	HFIR	0–1.2	60–100	25	570	0.07
6	9Cr–2VWTa	bcc	HFIR	0–1.2	60–100	25	545	0.08
7	9Cr–2WV	bcc	HFIR	0–1.2	60–100	25	541	0.07
8	9Cr–2VWTa	bcc	LANSCE	0–10.2	60–160	25	552	0.07
9	Mod. 9Cr–1Mo	bcc	LANSCE	0–10.2	60–160	25	562	0.08
10	Fe-a	bcc	HFIR	0–0.79	60–100	25	213	0.26
11	Fe-b	bcc	HFIR	0–1.07	60–100	25	104	0.29
12	Nb	bcc	HFIR	0–0.37	60–100	25	240	0.21
13	V	bcc	HFIR	0–0.69	60–100	25	304	0.19
14	316-a	fcc	HFIR	0–0.78	60–100	25	234	0.56
15	316-b	fcc	HFIR	0–1.2	60–100	25	223	0.70
16	316LN	fcc	HFIR	0–1.2	60–100	25	277	0.54
17	EC316LN	fcc	LANSCE	0–10.7	60–160	25	290	0.48
18	HTUPS316	fcc	LANSCE	0–10.7	60–160	25	179	0.37
19	AL6XN	fcc	LANSCE	0–10.7	60–160	25	279	0.48
20	Cu	fcc	HFIR	0–0.92	60–100	25	39	0.30
21	Ni	fcc	HFIR	0–0.6	60–100	25	63	0.42
22	Zr-4-a	hcp	HFIR	0–0.8	60–100	25	396	0.13
23	Zr-4-b	hcp	LANSCE	0–24.6	60–160	25	386	0.11
24	Zr	hcp	HFIR	0–0.63	60–100	25	44	0.35

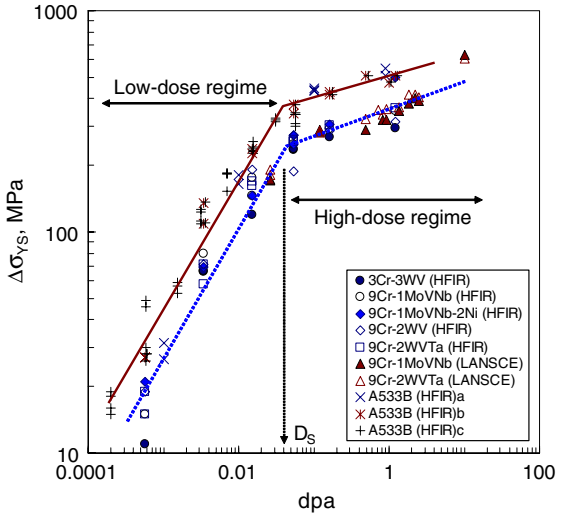

Fig. 1. Dose dependence of irradiation hardening in 3Cr, 9Cr, and A533B steels.

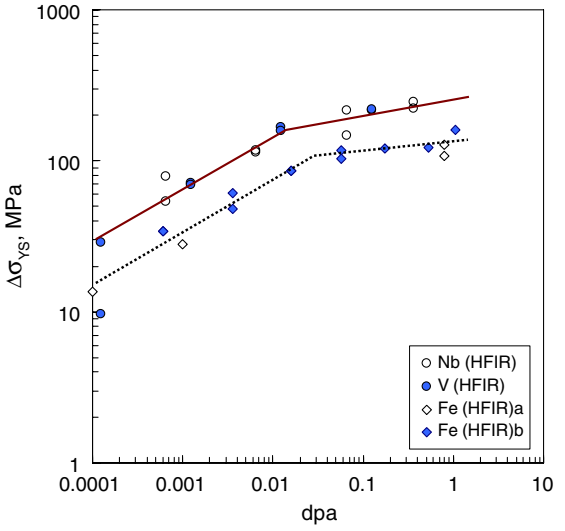

Fig. 2. Dose dependence of irradiation hardening in bcc pure metals.

of a big difference in their initial yield stresses, about 100 MPa for the high-purity Fe (Fe-b case) and about 210 MPa for the Fe-a case. This similarity in irradiation hardening behaviors of Fe metal with different purities produced a sharp contrast to the result [20] that the doses to plastic instability at yield, D_C, were very

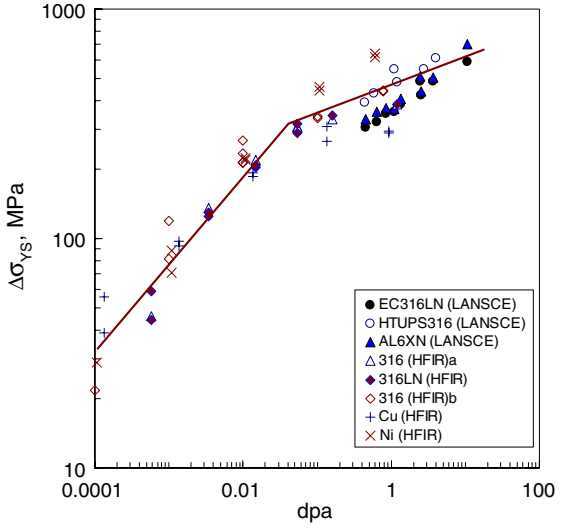

Fig. 3. Dose dependence of irradiation hardening in fcc alloys and pure metals.

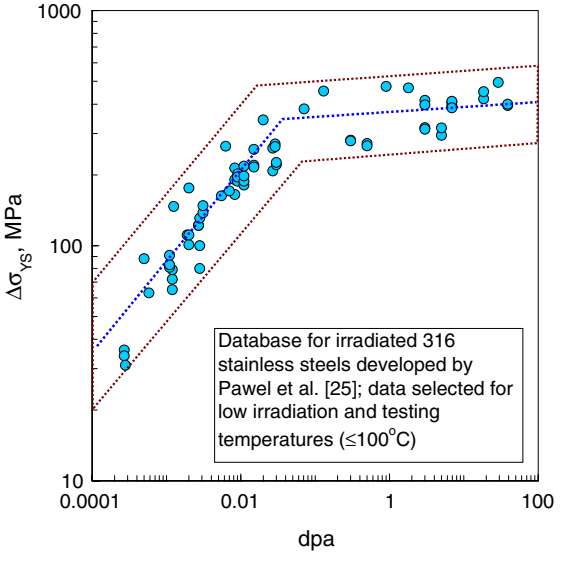

Fig. 4. Trend band for the increase in yield stress of 316 stainless steels; data selected for low irradiation and testing temperatures ($\leqslant 100$ °C) from the 316 database for fusion materials program [25].

different for those two cases, 6 dpa for the high-purity Fe and 0.2 dpa for the other case. The dose parameter D_C is defined as a minimum dose to have zero uniform ductility; above which the material will deform in a necking mode after yield [20]. As for the high-purity Fe, the n value was evaluated at a relatively low value of 0.26 for the low-dose regime. Also, it is noted that Nb and V behave alike in irradiation hardening. The dose

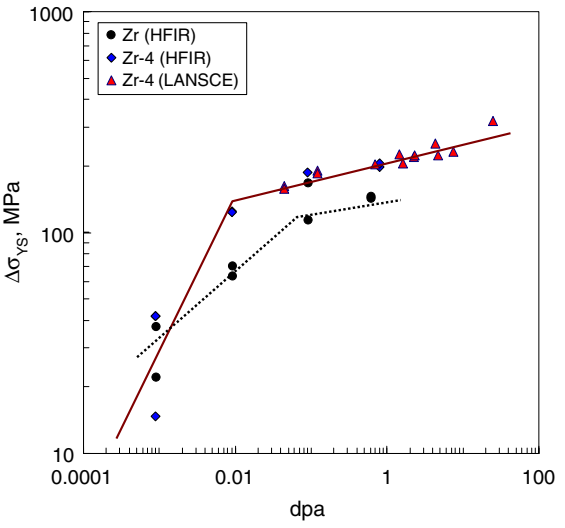

Fig. 5. Dose dependence of irradiation hardening in Zr-4 and pure metals.

dependencies were rather close to those of 3Cr and 9Cr steels; however, their transitions to the saturation regime occurred at a much smaller dose of 0.003 dpa.

The dose dependencies of irradiation hardening in the fcc metals are seen in Figs. 3 and 4. Their n values were in the range 0.31–0.48 in the low-dose regime and 0.01–0.24 in the high-dose regime; the average for the low-dose regime, 0.4, was slightly lower than that for bcc metals, 0.55. Also, a trend band for 316 stainless steels irradiated and tested at low temperatures ($\leqslant 100$ °C) was obtained from the database for 316 stainless steels [25] and is displayed in Fig. 4, in which tensile data from more than 15 experiments were integrated. The dose dependence found in Fig. 4 was similar to those of various austenitic stainless steels in the present study; the n values for the database were 0.38 and 0.04 for the low-dose and high-dose regimes, respectively. The D_S value was determined to be 0.04 dpa for Ni and stainless steels and 0.05 dpa for Cu. It is worth recalling that the D_C values for fcc metals were strongly material-dependent and ranged widely from about 0.2 dpa for Ni and Cu to 40 dpa for 316LN stainless steel [20].

Fig. 5 shows the dose dependence of irradiation hardening for pure Zr and Zr-4 alloy. Relatively-low n values were obtained for the pure Zr: 0.35 for the low-dose regime and 0.02 for the high-dose regime, whereas the values for Zr-4, 0.62 and 0.11 for the two regimes, were rather close to those of 3Cr and 9Cr steels.

Usually, the exponent n for the low-dose regime has been taken to represent irradiation-hardening behavior before reaching saturation. As given in Table 3, the average of all n values measured in the low-dose regime in this study is 0.5, which is the same as the theoretical value from barrier hardening models, assuming that the

Table 3
Summary for dose dependence of irradiation hardening

Case no.	Materials	Dose range (dpa)	D_S (dpa)	Dose $\leqslant D_S$		Dose $\geqslant D_S$	
				h	n	h	n
1	A533B-a	0–0.89	0.05	2300	0.62	530	0.08
2	A533B-b	0–1.2	0.03	2200	0.56	510	0.11
3	A533B-c	0–1.28	0.03	2710	0.58	510	0.14
4	3Cr–3WV	0–1.2	0.05	1590	0.62	290	0.07
5	9Cr–1MoVNb	0–1.2	0.03	1850	0.60	350	0.11
6	9Cr–2WVTa	0–1.2	0.04	1740	0.60	360	0.11
7	9Cr–2WV	0–1.2	0.04	1230	0.54	320	0.11
8	9Cr–2WVTa	0–10.2	0.04[a]			370	0.17
9	9Cr–1MoVNb	0–10.2	0.04[a]			350	0.18
10	Fe-a	0–0.79	0.05[a]	240[a]	0.26[a]	150[a]	0.11[a]
11	Fe-b	0–1.07	0.05	240	0.26	150	0.11
12	Nb	0–0.37	0.003	1970	0.52	280	0.18
13	V	0–0.69	0.003	4510	0.62	280	0.13
	Average for bcc group:				0.55[b]		0.12[b]
14	316-a	0–0.78	0.04[a]	2230	0.48	460	0.15
15	316-b	0–1.2	0.04	1060	0.40	380	0.07
16	316LN	0–1.2	0.04	1020	0.39	390	0.08
17	EC316LN	0–10.7	0.04[a]			360	0.22
18	HTUPS316	0–10.7	0.04[a]			480	0.18
19	AL6XN	0–10.7	0.04[a]			380	0.24
20	Cu	0–0.92	0.05	710	0.31	290	0.01
21	Ni	0–0.6	0.04	1660	0.44	700	0.19
	Average for fcc group:				0.40		0.14
	316 database	0–39	0.04	1120	0.38	370	0.04
22	Zr-4-a	0–0.8	0.01	2350	0.62	210	0.11
23	Zr-4-b	0–24.6	0.01[a]			210	0.07
24	Zr	0–0.63	0.07	350	0.35	150	0.02
	Average for hcp group:				0.49		0.07
	Average for whole group:				0.50		0.12

[a] Values are adopted from another case of the same or similar composition because of insufficient number of data for the case.
[b] 0.58 and 0.13, respectively, excluding the values for Fe cases.

production of stable defect clusters is proportional to dose [4,6,9]. However, it is also noted that some of the pure metals have lower n values than others; those values, 0.26, 0.31, and 0.35 for Fe, Cu, and Zr, respectively, are rather closer to 1/4 or 1/3 than to 1/2. In this low-dose regime, the exponent n has been measured at about 1/2 for many metals [4,9,15] and 1/4–1/3 for Cu and Au [12,15,16].

Detailed studies on irradiation-hardening behavior have been performed for Cu [16,17,26–34], and various exponent values have been reported. The exponents measured were either 1/3 [26] or 1/2 [26–30]. It has also been proposed that $n = 1/4$ is the appropriate dose exponent for Cu [31,32]. Zinkle and coworkers [16,17,33,34] showed that the defect-cluster density in pure Cu was initially linearly proportional to fluence at low doses ($\leqslant 0.0001$ dpa) and exhibited a square-root dependence before saturation. Consequently, the hardening exponent should change from 1/2 to 1/4 at a dose of $\sim$0.0001 dpa. The exponent should be lowered again due to a saturation of defect-number density at a higher dose. This change corresponds to the transition from the low-dose regime to the high-dose regime in the present study. It was also stated that the change from linear to square root behavior in defect-cluster density was dependent on impurity level [17]. Considering the significant amount of impurities in the current Cu specimens (see Table 1), the change might occur at a dose higher than the lowest dose of 0.0001 dpa in this irradiation experiment, and therefore, the hardening curve could be a combination of the curves with exponents of 1/4 and 1/2. Although the data points are too few to render the change precisely visible, the measured exponent, 0.31, for Cu seems reasonable. It is believed that the above discussion on the irradiation-hardening behavior of Cu can be applied to the other high-purity

metals, Fe and Zr, as well. It is also noted that the lower purity metals, V, Nb, and Ni, exhibited dose dependencies closer to 1/2, which is believed to be a common exponent for alloys in the low-dose regime. More systematic study is needed to explain fully the role of impurity and alloying atoms in defect-cluster accumulation and irradiation hardening.

3.2. Irradiation hardening and deformation parameters

It is well known that irradiation increases the tendency for premature plastic instability during tensile testing, and many metallic materials show prompt necking at yield after significant irradiation, with a subsequent negative slope in the engineering strain–stress curve [14,21,35,36]. This early plastic instability is often blamed on the softening effect from the clearance of radiation-induced defect clusters by the initial glide dislocations as well as on the reduction of irradiation-hardening rate [8,14,36–38]. However, it has recently been shown that prompt necking at yield is caused not by the softening effect but by the high yield stress exceeding the dose-independent plastic instability stress of the material [20]. When the strain-hardening rates before and after irradiation are compared at the same true stress level, they are very similar; at least, there is no sign of reduction in true strain-hardening rate by irradiation. This observation suggests that the apparently reduced strain-hardening rate after irradiation is directly related to the high stress, low strain-hardening rate portion of the stress–strain curve of unirradiated material. This tends to disapprove the hypothesis that the reduced strain-hardening rate should be related to the dose dependence of irradiation hardening. Elucidating a relationship between the irradiation-induced hardening and plastic instability behavior is attempted below. Also, that behavior is related to the deformation mechanisms and number-density of defect clusters.

An effective way to describe the radiation-induced behavior may be to make a comparison of the dose to saturation in irradiation hardening, D_S, with the dose to plastic instability at yield, D_C. Fig. 6 compares those two parameters. They exhibit a one-to-one proportionality ($D_C = D_S$) for doses up to ~0.05 dpa; at higher doses, D_S shows a saturation in the range 0.04–0.07 dpa. Pure bcc metals, V and Nb, showed low D_C and D_S values below 0.01 dpa [4]. (Although its data are excluded in this paper, the metal that showed the lowest critical doses was molybdenum [37]. It was not possible to evaluate the dose parameters for Mo because of immediate grain boundary embrittlement at the lowest dose of 0.0001 dpa in this experiment.) Zr-4 was also among the metals showing low D_C and D_S values, whereas the pure Zr showed the highest D_S value of 0.07 dpa. Data for A533B and the 3Cr and 9Cr steels are located at around the knee of the band. Data for Fe and the fcc metals

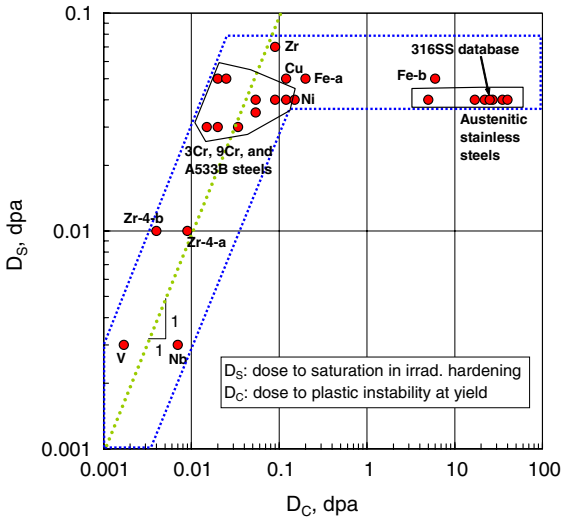

Fig. 6. Relationship between the doses to saturation in irradiation hardening and to plastic instability at yield.

(austenitic stainless steels, Ni, and Cu) fell in the near-horizontal band. A data point ($D_C = 25$ dpa, $D_S = 0.04$ dpa) for the tensile data in the 316 stainless steel database [25] is indicated in Fig. 6. No fcc metal showed a D_S value below 0.04 dpa.

Except for the high-purity Fe (Fe-b), the data for bcc and hcp metals were within the experimental error bounds at both sides of the $D_C = D_S$ line. This result suggests that saturation in irradiation hardening and plastic instability at yield often start at similar doses. Since several metals are involved, the concurrence of the two events cannot be interpreted as a one-time incident that both phenomena happen to occur at similar doses without any inter-relationship. The concurrence of the two events may be possible if the plastic instability at yield occurs before saturation in defect-cluster density, which is also directly related to the saturation in irradiation hardening. A possible interpretation for the equality ($D_C = D_S$) is that the plastic instability at yield has reduced the increasing rate of yield stress due to irradiation, leading the irradiation hardening to a saturation in the high-dose regime. For all cases, D_S has not exceeded D_C, within experimental error. This indicates that the extension of the low-dose regime in irradiation hardening was stopped by the plastic instability at yield. A question is how the plastic instability affected the yielding process before which the elastic behavior supposedly governed the deformation. A clue for an explanation can be the local micro-strain occurring before macroscopic yielding. The micro-strain occurs in a narrow strain range before the macroscopic yielding [39]. Its contribution to the macroscopic strain is limited. If an irradiated tensile specimen is loaded to a stress level just below its apparent yield stress but above its

plastic instability stress, local plastic deformation might occur in a microscopically high-stress region of the specimen around the strongest stress concentrator. The plastic deformation in the high-stress region must be subjected to a plastic instability condition because the stress is above the instability stress of the material. In such a situation, the ability to increase macroscopic stress by elastic deformation should be reduced. Since the local plastic instability may lead to a more severe stress concentration, the macroscopic stress cannot continue to increase, but it will decrease as the localized strain propagates into the entire specimen cross section, showing apparent macroscopic yielding. After the yielding process, strain hardening might resume if the stress has decreased below the plastic instability stress.

If the high-dose regime in irradiation hardening of the bcc and hcp metals is due to a plastic instability, deformation in this regime should be prone to producing channels at doses around their D_S values, because the plastic instability always occurs at a reduced strain-hardening rate. The lowest doses at which channel deformation has been observed are: 0.007 dpa for Nb [4]; 0.01–0.05 dpa for Zr-2 and Zr-4 [22,40]; ~0.001 for V and ~0.1 [41] for A533B [22]. These doses are similar to the D_S and D_C values for those metals. Therefore, three phenomena: prompt plastic instability at yield, dislocation channeling, and the transition between the low-dose to the high-dose regimes in irradiation hardening, seem to occur at similar doses in many bcc and hcp metals with alloying elements or high impurities. However, the concurrence of multiple phenomena cannot be generalized for all metals. Highly ductile metals, especially fcc metals, show those phenomena occurring at different doses, as described below.

In the fcc metals and high-purity Fe, the saturation of irradiation hardening (in yield stress) always occurred at doses lower than the doses to plastic instability at yield; i.e., $D_S < D_C$. It is remarkable that the D_C values for stainless steels and high-purity Fe are 2 to 3 orders of magnitude higher than their D_S values, in the range 0.04–0.05 dpa. This indicates that in those metals the saturation in irradiation hardening occurs well before the metals experience plastic instability at yield, so the transition from low-dose to high-dose regime is less affected by the plastic instability. A mechanism that can initiate the transition may be channel deformation. For Cu, many investigators have reported that channel deformation occurs after irradiation to doses above 0.01 dpa [29,42]. Further, the channel deformation in stainless steels seemed to occur at similar doses (>~0.1 dpa) as the D_S value, 0.04 dpa [22]. In some experiments, however, channel deformation has been observed at much lower doses: 0.0005–0.004 dpa in Cu [43–46], 0.002–0.02 dpa in Ni [15,47], and 0.0025–0.4 dpa in Fe [42,48]. (A fluence to dpa ratio of 6×10^{24} nm^{-2}/dpa was used in conversion from fast neutron fluence ($E > 1$ MeV) to dpa.) It seems that the dose to channel deformation is dependent on the material condition, such as impurity level, whereas the irradiation hardening behavior is less sensitive to the material condition, as implied in Figs. 1–5. For example, the high- and low-purity irons showed almost the same dose dependence in hardening behavior in Fig. 2. However, the generalization of this observation might require more evidence on a larger variety of material conditions. Also, it is interesting to note that the highly ductile metals deformed in a channeling mode when the strain-hardening rate was high and the strain level was well below the plastic instability strain [15,23]. Therefore, we can conclude that the occurrence of channel deformation is not always consistent with plastic instability at yield or with a change in the regime of irradiation hardening.

Although neither plastic instability at yield nor channel deformation can account for the transition from a low-dose to a high-dose regime in highly-ductile metals, another phenomenon that can cause the transition is the saturation of defect-cluster density [16,17]. Two reasons for the saturation of defect-cluster density have been suggested on the basis of cascade simulation results [18]: (1) as the inter-defect spacing becomes smaller, it is more likely that the defects in the next cascade will react with existing clusters at the expense of new clusters, and (2) it becomes more likely that the next cascade will occur on the top of existing defects and will erase them. Both effects from overlap of cascades might result in fewer net defects [18,19]. Since irradiation hardening is presumed to be proportional to the defect-cluster density, its saturation, or reduced accumulation rate at high doses, should result in similar behavior in irradiation hardening. A number of investigations on defect microstructures have shown that the defect cluster density in fcc metals increases with dose and reaches a saturation level in the dose range 0.01–0.1 dpa at low temperatures [16,33,34,37,49]. Among the fcc metals the most widely studied ones for defect accumulation behavior are Cu and its alloys [16,17,33,34,37,49–52]. In Cu, the accumulation of defect clusters (mostly stacking fault tetrahedra) at low temperatures (<~300 °C) was found to be linear with dose at low doses below 0.0001 dpa and to have a square-root dependence on dose in the range 0.0001–0.1 dpa, followed by a saturation at doses above ~0.1 dpa [17]. In Ni, saturation was reached after irradiation to doses above 0.1 dpa, although the visible defect density was 5–10 times lower than that in Cu [33,37]. Further, the results of transmission electron microscopy (TEM) and positron annihilation spectroscopy (PAS) showed that the dose dependence of defect-cluster density for Fe-b (high purity Fe) was similar to that for Cu, although the defect-cluster density was at least one order of magnitude lower than that of Cu [52]. In the Fe-b the defect density continued to increase with dose over the test dose range of 0.0001–0.72 dpa;

however, it showed near saturation above 0.1 dpa. In stainless steels, the doses needed to approach the saturation of defect cluster density were in the range 0.1–1 dpa [51,53]. Therefore, a dose of about 0.1 dpa should be a common dose for the saturation of defect cluster density in fcc metals and high-purity Fe. Since the strength of a material under barrier-hardening model cannot continue to increase rapidly without rapid accumulation of defect clusters, a dose of 0.1 dpa must be a ceiling dose to the low-dose regime in the radiation-induced hardening; this is consistent with the observation that the doses at the transition between the low-dose to the high-dose regimes are in the range 0.03–0.07 dpa, as shown in Fig. 6. Based on the above discussion, it is suggested that the transition between the low-dose to the high-dose regimes occurs (1) when the tensile specimen undergoes plastic instability before yield or (2) when the defect-cluster density approaches a saturation level.

3.3. Irradiation hardening and onset of channeling

The fact that channeling can occur at a dose well below D_S supports the finding in Ref. [20] that the true stress–true strain curve, if compared at the same true stress, is not significantly changed by irradiation; this also indicates that the channel deformation does not change the post-yield true strain-hardening behavior of polycrystals even though it may appear to reduce the engineering strain-hardening rate. Although channel deformation is believed to be evidence of localized deformation, with background contrast from removable defects, this does not necessarily mean negative strain hardening. Further, a numerical simulation showed that a back stress of similar magnitude to the applied stress could be developed at the edge of a channel [54]. Since the back stress is a key component of the strain-hardening stress, the hypothesis that channel deformation can induce strain softening, the underlying meaning of which is a negative strain-hardening rate, may be incorrect.

Although the detailed mechanism of channel formation is largely unknown, some of the dislocations formed during channeling may form pileups against strong obstacles, such as grain boundaries, without being transferred to an adjacent grain, and the back stress due to the dislocation pileups might stop further slip in the channel [54,55]. A drop of shear stress in the channel may occur in the early stage of channel formation. However, the stress should recover quickly to the stress level in the adjacent regions as the back stress builds up. Also, the volume fraction of channels under formation is small, thus the overall contribution by the developing channels to macroscopic stress may not be more significant than that due to formation of any deformation band without irradiation defects (for example, a Lüders band). Actually, as long as channel formation spreads to another region, the local strain-hardening rate cannot be negative. Negative strain hardening cannot give rise to a diffusion of plastic deformation, and should cause immediate failure without large necking ductility. However, most of the tested metals retained significant necking ductility, even with prompt necking at yield. Further, no negative slope in the true stress–true strain curve has been calculated for the necking deformation after significant irradiation [23,35]. Positive macroscopic strain hardening with localized deformation was also reported for pre-strained Cu single crystals [56,57]. It was also shown by an elastic energy theory that localized deformation can occur in dispersion-hardened materials if any work-softening obstacles are contained in the materials; negative macroscopic strain-hardening rate is not required for strain localization [58]. Therefore, although more studies are needed for generalization, channeling (or localized deformation) is believed to be a common phenomenon for high-stress deformations; it occurs more easily when the strain-hardening rate is much reduced from the pristine condition of the material. So, whether the saturation in irradiation hardening occurs simultaneously with channel deformation or not seems to depend on the material properties, especially on the ductility and strain-hardening capability before irradiation.

4. Conclusions

Irradiation-hardening behaviors have been investigated for bcc, fcc, and hcp metals after low-temperature (<200 °C) irradiations. The following conclusions were drawn:

(1) The log–log plots of $\Delta\sigma_{YS}$ vs. dpa data showed two distinct regimes: a low-dose regime and a high-dose regime. Regression analysis was performed for those regimes using a power-law function $\Delta\sigma_{YS} = h(\text{dpa})^n$. Mean values for n obtained from the 19 metals were about 0.5 for the low-dose regime and about 0.12 for the high-dose regime. Some pure metals like Fe, Cu, and Zr displayed lower values.

(2) The doses to saturation in irradiation hardening, D_S, were in the range 0.003–0.07 dpa, and were compared with their doses for the onset of prompt plastic instability at yield, D_C. Most bcc and hcp metals had data falling within the bounds for the $D_C = D_S$ line up to ~0.05 dpa. The D_C values for pure Fe, Zr, and fcc metals formed a horizontal band with a dose span of 0.04–0.07 dpa.

(3) The transition between the low-dose to the high-dose regimes in irradiation hardening seems to occur either when the tensile specimen undergoes plastic instability at yield or when a saturation of defect-cluster density is reached.

(4) Although channel deformation is common at doses around D_S (or D_C), it is not necessarily the cause of plastic instability at yield or the approach to saturation in irradiation hardening. It seems to be more a result of the higher stress associated with irradiation hardening.

Acknowledgements

This research was sponsored by US Department of Energy, Offices of Fusion Energy Sciences and Basic Energy Science, under Contract DE-AC05-00OR22725 with UT-Battelle, LLC. The authors express special thanks to Drs S.J. Zinkle, J.G. Merkle and R.L. Klueh for their technical reviews and thoughtful comments.

References

[1] F.A. Smidt Jr., NRL Report 7078, Naval Research Laboratory, Washington, DC, 1970.
[2] R.L. Sindelar, Reactor materials program – microstructural and mechanical response of types 304, 304L, and 308 stainless steels to low temperature neutron irradiation (U), WSRC-TR-93-196 TASK 89-023-1, Savannah River Tech. Center, Aiken, SC 29808, Westinghouse Savannah River Company, 1993.
[3] C.E. Ells, C.D. Williams, Trans. JIM 9 (1968) 214.
[4] R.P. Tucker, M.S. Wechsler, Radiat. Eff. 3 (1970) 73.
[5] M.J. Makin, F.J. Minter, Acta Metall. 8 (1960) 691.
[6] K.L. Murty, D.J. Oh, Scr. Metall. 17 (1983) 317.
[7] B.N. Singh, A.J.E. Foreman, H. Trinkaus, J. Nucl. Mater. 249 (1997) 103.
[8] R.R. Hosbons, C.E. Coleman, R.A. Holt, Numerical simulation of tensile behavior of nuclear cladding materials, AECL-5245, Chalk River Nuclear Laboratories, Chalk River, Ontario, Canada, 1975.
[9] A.K. Seeger, in: Proceedings of the 2nd Int. Conf. on Peaceful Uses of Atomic Energy, vol. 6, 1958, p. 250.
[10] A.H. Cottrell, R.J. Stokes, Proc. R. Soc. A 233 (1955) 17.
[11] P.M. Kelly, Int. Metal. Rev. 18 (1973) 31.
[12] T.H. Blewitt, R.R. Coltman, R.E. Jamison, J.K. Redman, J. Nucl. Mater. 2 (1960) 277.
[13] D.K. Holmesin, Solid State Division Annual Progress Report, ORNL-2413, Oak Ridge National Laboratory, Oak Ridge, TN, November 1957, p. 13.
[14] K. Farrell, T.S. Byun, J. Nucl. Mater. 318 (2003) 274.
[15] A. Okada, T. Yoshiie, S. Kojima, M. Kiritani, J. Nucl. Mater. 141–143 (1986) 907.
[16] S.J. Zinkle, J. Nucl. Mater. 150 (1987) 140.
[17] S.J. Zinkle, Radiat. Eff. Def. Solids 148 (1999) 447.
[18] H.L. Heinisch, B.N. Singh, J. Nucl. Mater. 271&272 (1999) 46.
[19] Y. Satoh, I. Ishida, T. Yoshiie, M. Kiritani, J. Nucl. Mater. 155–157 (1988) 443.
[20] T.S. Byun, K. Farrell, Plastic instability properties of polycrystalline metals after low temperature irradiation, Acta Mater., in press.
[21] K. Farrell, T.S. Byun, Tensile properties of candidate SNS materials after irradiation in two neutron areas in the LANSCE accelerator, SNS/TR-211, Oak Ridge National Lab., January 2001.
[22] K. Farrell, T.S. Byun, N. Hashimoto, Mapping flow localization processes in deformation of irradiated reactor structural alloys, Oak Ridge National Lab., ORNL/TM-2002/66, July 2002, and ORNL/TM-2003/63, July 2003.
[23] T.S. Byun, K. Farrell, E.H. Lee, L.K. Mansur, S.A. Maloy, M.R. James, W.R. Johnson, J. Nucl. Mater. 303 (2002) 34.
[24] R.L. Klueh, D.J. Alexander, J. Nucl. Mater. 187 (1992) 60.
[25] J.E. Pawel, A.F. Rowcliffe, D.J. Alexander, M.L. Grossbeck, K. Shiba, J. Nucl. Mater. 233–237 (1996) 202, and private discussion with J.E. (Pawel) Robertson.
[26] T.H. Blewitt, in: D.S. Billington (Ed.), Radiation Damage in Solids, Proc. Inst. School of Physics (Enrico Fermi) Course XVIII, Academic, London, New York, 1962, p. 630.
[27] J. Diehl, W. Schilling, in: Proceedings of the 3rd International Conference on Peaceful Uses of Atomic Energy, vol. 9, 1965, p. 72.
[28] M.J. Makin, in: W.F. Sheely (Ed.), Radiation Effects, vol. 37, TMS-AIME Conf. Asheville, NC, 1965, Gordon and Breach, New York, 1967, p. 627.
[29] T.J. Koppenaal, R.J. Arsenault, J. Inst. Metals 16 (1971) 175.
[30] B.L. Eyre, Int. Metall. Rev. 19 (1974) 240.
[31] S.J. Zinkle, G.L. Kulcinski, J. Nucl. Mater. 122&123 (1984) 449.
[32] H.L. Heinisch, S.D. Atkin, C. Martinez, J. Nucl. Mater. 141–143 (1986) 807.
[33] S.J. Zinkle, L.L. Snead, J. Nucl. Mater. 225 (1995) 123.
[34] B.N. Singh, S.J. Zinkle, J. Nucl. Mater. 206 (1993) 212.
[35] E.V. van Osch, M.I. DeVries, J. Nucl. Mater. 271&272 (1991) 162.
[36] A. Luft, Prog. Mater. Sci. 35 (1991) 97.
[37] B.N. Singh, J.H. Evans, A. Horsewell, P. Toft, G.V. Müller, J. Nucl. Mater. 258–263 (1998) 865.
[38] R.B. Adamson, S.B. Wisner, R.P. Tucker, R.A. Rand, in: W.R. Corwin, G.E. Lucas (Eds.), The Use of Small Specimens for Testing Irradiated Material, ASTM STP 888, American Society for Testing and Evaluations, Philadelphia, 1986, p. 171.
[39] T. Onchi, H. Kayano, Y. Higashiguchi, J. Nucl. Mater. 88 (1980) 226.
[40] Y. Huang, R.J. Arsenault, Radiat. Eff. 17 (1973) 3.
[41] N. Hashimoto, T.S. Byun, K. Farrell, S.J. Zinkle, Deformation microstructure of neutron-irradiated pure poly crystalline vanadium, Acta Metall., submitted for publication.
[42] B.N. Singh, A. Horsewell, P. Toft, J. Nucl. Mater. 271&272 (1999) 97.
[43] J.V. Sharp, Acta Metall. 22 (1974) 449.
[44] J.V. Sharp, Philos. Mag. 16 (1967) 77.
[45] H. Neuhäuser, R. Rodloff, Acta Metall. 22 (1974) 375.
[46] E. Johnson, M.J. Goring, in: B. Joaffrey, P. Fauard (Eds.), Radiation Hardening Effects in Neutron Irradiated Cooper Observed In Situ in the High Voltage Microscope, HVEM 4, 1975, French Electron Microscopy Society, Toulouse, France, 1975, p. 317.

[47] N. Noda, H. Saka, K. Shiraishi, H. Yoshida, T. Imura, In-situ studies on dynamic formation of dislocation channels in neutron-irradiated Ni by HVEM, in: T. Imura, H. Hashimoto (Eds.), Proceedings of the Fifth Int. Conf. on High Voltage Electron Microscopy, Jpn. Soc. Electron Microscopy, Tokyo, Japan, 1977, p. 403.
[48] H. Mughrabi, D. Ströhle, M. Wilkens, Z. Metall. 72 (5) (1981) 300.
[49] M.J. Caturla, N. Soneda, E. Alonso, B.D. Wirth, T. Díaz de la Rubia, J.M. Perlado, J. Nucl. Mater. 276 (2000) 13.
[50] M. Victoria, N. Baluc, C. Bailat, Y. Dai, M.I. Luppo, R. Schäublin, B.N. Singh, J. Nucl. Mater. 276 (2000) 114.
[51] S.J. Zinkle, P.J. Maziasz, R.E. Stoller, J. Nucl. Mater. 206 (1993) 266.
[52] M. Eldrup, B.N. Singh, S.J. Zinkle, T.S. Byun, K. Farrell, J. Nucl. Mater. 307–311 (2002) 912.
[53] E.H. Lee, J.D. Hunn, T.S. Byun, L.K. Mansur, J. Nucl. Mater. 280 (2000) 18.
[54] J. Gittus, Irradiation Effects in Crystalline Solids, Applied Science, 1978, p. 197.
[55] M.J. Makin, J.V. Sharp, Phys. Stat. Sol. 9 (1965) 109.
[56] Z.S. Basinski, P.J. Jackson, Phys. Stat. Sol. 9 (1965) 805.
[57] Z.S. Basinski, P.J. Jackson, Phys. Stat. Sol. 10 (1965) 45.
[58] T. Mori, T. Mura, Mater. Sci. Eng. 26 (1976) 89.